Applied Problems of Nonlinear Oscillation and Wave Theory

Izvestiya Vysshikh Uchebnykh Zavedeniy. Applied Nonlinear Dynamics. 2023;31(3)

Article DOI: 10.18500/0869-6632-003042

Spatial and temporal dynamics of the emergence of epidemics in the hybrid SIRS+V model of cellular automata

A. V. Shabunin

Saratov State University, Russia
E-mail: shabuninav@info.sgu.ru

Received 29.01.2023, accepted 21.03.2023, available online 3.05.2023, published 31.05.2023

Abstract. *Purpose* of this work is to construct a model of infection spread in the form of a lattice of probabilistic cellular automata, which takes into account the inertial nature of infection transmission between individuals. Identification of the relationship between the spatial and temporal dynamics of the model depending on the probability of migration of individuals. *Methods.* The numerical simulation of stochastic dynamics of the lattice of cellular automata by the Monte Carlo method. *Results.* A modified SIRS+V model of epidemic spread in the form of a lattice of probabilistic cellular automata is constructed. It differs from standard models by taking into account the inertial nature of the transmission of infection between individuals of the population, which is realized by introducing a "carrier agent" into the model, which viruses act as. The similarity and difference between the dynamics of the cellular automata model and the previously studied mean field model are revealed. *Discussion.* The model in the form of cellular automata allows us to study the processes of infection spread in the population, including in conditions of spatially heterogeneous distribution of the disease. The latter situation occurs if the probability of migration of individuals is not too high. At the same time, a significant change in the quantitative characteristics of the processes is possible, as well as the emergence of qualitatively new modes, such as the regime of undamped oscillations.

Keywords: population dynamics, SIRS model, dynamical systems.

For citation: Shabunin AV. Spatial and temporal dynamics of the emergence of epidemics in the hybrid SIRS+V model of cellular automata. Izvestiya VUZ. Applied Nonlinear Dynamics. 2023;31(3):271–285. DOI: 10.18500/0869-6632-003042

Introduction

The practical application of nonlinear dynamics is based on the construction of mathematical models of natural phenomena and technical devices that allow predicting their behavior, including when changing external conditions. One of such tasks is modeling the processes of spreading epidemics of infectious diseases in biological populations [1–4].

Mathematical modeling of epidemics is carried out by different methods: by analyzing time series [5], constructing regression [6] and autoregressive [7] models, the use of systems of ordinary differential equations [8], partial differential equations [9], as well as lattices of cellular automata [10–13]. The classical approach to modeling is to divide the population into groups of individuals and determine the rules of interaction for them, from which by means of averaging, equations are obtained for the observed quantitative characteristics of the disease.

An example of this approach is *SIRS*, a model proposed in the 1920s by Kermack and McKendrick [8]. In this model, the population is divided into three classes: healthy and susceptible (S—**S**usceptible), sick (I— **I**nfectious) and recovered (R— **R**ecovered) individuals. Interaction rules are defined for them (occurring during the time interval Δt):

- a meeting of a susceptible individual (S) with an infected one (I) leads with probability P_1 to infection of a susceptible individual: $S + I \xrightarrow{P_1} 2I$;
- a diseased individual (I) with a probability of P_2 is cured, while acquiring immunity to subsequent infections (R): $I \xrightarrow{P_2} R$;
- an immune individual (R) with a probability of P_3 loses immunity, returning the individual to a susceptible state (S): $R \xrightarrow{P_3} S$.

Thus, in the evolution of each individual, we observe a cyclic chain of transformations between a discrete and a finite set of states $S \to I \to R \to S$. Hence the name of this model — *SIRS*. In the SIRS model , the infection rate is determined by the frequency of contacts between susceptible and infected individuals. This rule was first proposed in the work [14] and was widely used in the future. However, it does not always adequately describe the actual infection processes that they can be characterized by both non-locality and inertia. This is typical for respiratory viral infections, when the virus causing infection can exist outside the host body for a long time. Therefore, the act of infection can occur in isolation (in time and space) from direct contact between S and I individuals. This requires adding additional inertia to the model in the form of a lagging argument [15–17], or, as it was done in [18], using an additional variable (and, accordingly, an additional equation).

In the work [18], a modification of the SIRS model was proposed, in which the transmission of infection occurs indirectly, due to the interaction of a susceptible individual with a carrier agent, which is viruses. This model will be referred to as the *SIRS+V* model in the future. SIRS+V is a model of interaction between two systems: a population of individuals and a population of viruses, each of which lives according to its own laws. Individuals — these are isolated individuals whose condition changes in a discrete way. Viruses form, as it were, an external field affecting on individuals and leading to a change in their condition — infection.

In [18] SIRS+V, the model was investigated using the ODE system (that is, in the mean field approximation) and demonstrated a qualitative correspondence with the dynamics of real epidemic processes. However, the approximation of the mean field is a very crude idealization for epidemic processes, since spatial heterogeneity can be a determining factor for them. Therefore, in this study, we decided to investigate this model using the *probabilistic cellular automata* (PCA) method, which allow us to simulate processes infection/recovery at the level of individual individuals, taking into account their probabilistic nature, as well as to investigate emerging spatial structures.

A cellular automaton (CA) is a system (cell) that has a finite set of states. Switching

between them occurs discretely in time according to a given law [19, 20]. If the law of change of cell states is a stochastic Markov process, then such CA is called probabilistic, otherwise — deterministic. Cellular automata are combined into networks (lattices). Lattices of cellular automata (LCA) are a powerful tool for modeling physical processes in distributed systems, they allow us to obtain their temporal and spatial dynamics [21]. Oscillatory and wave phenomena characteristic of dynamical systems are observed in them : periodic, quasi-periodic and chaotic oscillations [22, 23], propagation of waves and wave fronts [24].

PCA models have an advantage over ODE, since they allow us to consider spatially heterogeneous disease processes and allow us to investigate the role of migration processes on the course of the disease. For example, in the works [10, 25] it was shown that the use of medium field models is justified only with high migration of individuals, when there is a strong mixing of infected individuals in space. With weak migration, when the infection is of a focal nature, the predictions of the ODE and PCA models differ greatly. Subsequently, this conclusion was confirmed in [12]. In [11], the PCA method was used to assess the role of vaccination on the epidemic development processes. In all these works , modeling was carried out on the basis of the classical SIRS algorithm. In this study, the method of probabilistic cellular automata is used for the modified SIRS+V algorithm.

1. SIRS+V model of the spread of infectious diseases

In the standard SIRS model, the act of infection is described as the result of local contact of S and I individuals: $S + I \to 2I$. However, in practice, infection can also occur indirectly, without direct interaction of individuals. In the modified system , exactly such an infection scheme is proposed, based on the interaction of individuals with viral particles, hereinafter referred to as V. In this scheme, a sick individual (I) acts as a generator of viruses (V), which , due to diffusion, spread in space, infecting susceptible individuals (S) : $S \overset{P_1(v)}{\to} I$.

Thus, instead of the standard SIRS model, a two-component (individuals + viruses) model will be used: $S \overset{P_1(v)}{\to} I \overset{P_2}{\to} R \overset{P_3}{\to} S$. It takes into account that the probability of infection P_1 depends on the concentration of viruses (v) at the location of the individual. The function $P_1(v)$, following [18], selected as: $P_1(v) = 1 - \exp(-\alpha v)$, where $\alpha > 0$ is a factor characterizing the infecting ability of viruses. The probabilities P_2 and P_3 are constants, the values of which characterize the average duration of illness and loss of immunity (measured in the number of elementary intervals Δt): $\tau_2 = P_2^{-1}$ — the average duration of the disease (the so-called «infection period»), $\tau_3 = P_3^{-1}$ — the average duration of immunity.

In the SIRS+V model, the dynamics of viral particles is fundamentally different from the behavior of individuals in the population. The latter are particles with a discrete set of states $\{S, I, R\}$. Transitions between them are random events and are characterized by their probability values (P_k, $k = 1, 2, 3$). We believe that each of the individuals requires a certain habitat (let's call it *unit cell*). As a result, the number of individuals in a finite region is limited by the number of elementary cells N. In contrast due to this, viral particles can accumulate at every point in space. Therefore, their number can take arbitrary non-negative values[1].

The transformations that occurred in each elementary cell of space during the time Δt are

[1] The discrete nature of the number of viruses can be neglected, since it is incomparably huge compared to the number of individuals.

represented as the following scheme:

$$\begin{array}{lcll} S & \overset{P(v)}{\rightarrow} & I & \\ I & \overset{P_2}{\rightarrow} & R & (1) \\ R & \overset{P_3}{\rightarrow} & S & \\ I & \rightarrow & I + \sigma V & (2) \\ V & \rightarrow & (1-\mu)\, V, & \end{array}$$

where the first three reactions describe the modified SIRS scheme, and the last two define the law of virus change:

- an infected individual (I) generates σ of virus particles (V);
- part of viruses (μ) is inactivated.

The parameters σ and μ set the rates of virus production and removal. The first of them is determined by the ability of viruses to multiply inside the host organism, and the value inverse to μ determines the characteristic time of existence of the virus outside the body of an infected individual.

When considering the spread of the epidemic, the main interest is not the dynamics of individual individuals, but the change in their number N_k ($k \in \{S, I, R\}$). When studying the model , it is convenient to use their relative values instead of the values N_k: $s = N_S/N$, $i = N_I/N$, $r = N_R/N$, which we will call densities (concentrations) of the corresponding groups of individuals. Due to the immutability of the total population, the sum of $s + i + r$ is a constant value — the population density of the population, hereinafter referred to as C.

In addition to reactions that change the number of individuals and viruses, processes that change their distribution in space- migration - play an important role. By migration we mean random changes of individuals in their spatial coordinates (similar to the diffusion of Brownian particles). As a result , each of the individuals, regardless of its state $\{S, I, R\}$, moves in an arbitrary direction and at an arbitrary distance. Migration does not directly affect the values of N_k. However, it can affect on them indirectly, through a change in the spatial distribution of individuals. The migration process leads to a gradual mixing of individuals of different species in space. For viruses, migration is defined as local diffusion, in which there is a « virus current» from places with a high concentration to neighboring areas with a lower concentration.

2. SIRS+V model in the form of a lattice of cellular automata

The evolution of a single individual, which is set by the system (1), (5), is a ready-made set of rules for the functioning of a probabilistic cellular automaton. The population of individuals can be described as an ensemble of such automata. Let's define an ensemble in the form of a square lattice (matrix) $\hat{M}$, with the size of $L \times L$ cells. Each cell corresponds to an elementary cell of the population. A cell can take one of the values $\{S, I, R, E\}$. The first three values correspond to the state of the individual occupied by it. Last value (**E**mpty) corresponds to an empty cell. Total number of cells $N = L^2$ defines the maximum capacity of the population. The relative number of «non-empty» cells determines the previously entered parameter C. The position of the cell in the lattice is identified by two indexes: i — row number and j — column number of the matrix, which are associated with spatial coordinates. Thus, the state of the lattice cells $M_{i,j}$ ($i, j = 1, \ldots, L$) defines the spatial distribution of the population.

The evolution of the lattice of cellular automata takes place from the initial state $\hat{M}_0$

during a sequence of iterations

$$\hat{M}(t+1) = F(\hat{M}(t), \hat{V}(t)) \tag{3}$$

with discrete time t, where F is a stochastic operator implementing schemes (1), (5), $\hat{V}$ — matrix $L \times L$, specifying the spatial distribution of viruses. The equation (3) must be supplemented with the equation for $\hat{V}(t)$. Let 's write it down as a lattice of diffusionally connected maps

$$V_{i,j}(t+1) = g_{i,j}(t) + \frac{\gamma}{4}\Big(g_{i-1,j}(t) + g_{i+1,j}(t) + g_{i,j-1}(t) + g_{i,j+1}(t) - 4g_{i,j}(t)\Big), \tag{4}$$

where $g_{i,j}$ is a function describing the reactions of the scheme (2) at each point in space

$$g_{i,j} = V_{i,j} - \mu V_{i,j} + \sigma h(M_{i,j}),$$
$$h(M_{i,j}) = \begin{cases} 1, & M_{i,j} = I, \\ 0, & M_{i,j} \neq I; \end{cases}$$

the term in parentheses is a discrete analogue of the two-dimensional operator ∇ ([27, 28]); $\gamma \in [0 : 0.8]$— diffusion coupling coefficient.

3. Numerical simulation algorithm

To find the trajectory $\hat{M}(t)$, $t = 0, 1, \ldots$, it is necessary to find a numerical solution of the system (3), (4). The map (4)is solved by direct integration. To find the dynamics of the LCA (3) the following method is used: at each step of the discrete time t, the current states of all N elements of the lattice $M_{i,j}$ are determined. Then they are transformed according to the rules of the reactions of the scheme (1).

(a) If $M_{i,j} = S$, the state of the original cell with probability $P_1(v_{i,j})$ is transformed into I. This is how a random infection event is implemented.

(b) If $M_{i,j} = I$, the state of the original cell with probability P_2 is transformed into R, that is, a cure event is realized.

(c) If $M_{i,j} = R$, the state of the original cell with probability P_3 is transformed into S, that is, there is a loss of immunity and a return to the original state.

Transformations (a)–(c) are performed in random order and implement modeling of processes related to the disease.

There is migration in the dynamics of the LCA — a random change in the spatial coordinates of individuals. The result of such a displacement can be represented as a global diffusion reaction, in which two particles occupying different cells change places

$$X \overset{P_m}{\leftrightarrow} Y. \tag{5}$$

Here X and Y are individuals of any kind, including «vacancy», that is, an empty cell; P_m — probability.

We implement the described algorithm step by step and get the evolution of the lattice PCA in the form of a time dependence of the matrix $\hat{M}$. In Fig. 1 is an example of simultaneous «snapshots» matrices $\hat{M}$ and $\hat{V}$ for parameter values: $\alpha = 1$, $P_2 = 0.1$, $P_3 = 0.0033$, $\sigma = 0.7$, $\mu = 0.3$, $\gamma = 0.8$[2] and $P_m = 0.0001$. Here we observe a high correlation in the distribution of sick

[2]These parameter values will be used further.

individuals and the distribution of viruses, which persists in other cases. Due to the probabilistic For cellular automata, the dependencies $\hat{M}(t)$ and $\hat{V}(t)$ are random functions of time. However, after averaging over an ensemble of cells with a large N, the relative concentrations of individuals of each species

$$k = \frac{N_K}{N} \tag{6}$$

($K \in \{S, I, R\}$) will represent deterministic quantities. They are considered in the study.

4. Comparison of the PCA lattice with the mean field model

In the SIRS+V mean field approximation, the model (1) is described by a system of ordinary differential equations governing the change in concentrations of individuals ($i = N_I/N$, $r = N_R/N$) and viruses ($v = N_V/N$):

$$\begin{aligned} \dot{i} &= P(v)\,(C - i - r) - P_2 i, \\ \dot{r} &= P_2 i - P_3 r, \\ \dot{v} &= \sigma i - \mu v. \end{aligned} \tag{7}$$

A study conducted in [18] showed that the only attractor of the phase space (7) is an equilibrium state of the stable focus type. Therefore , the development The epidemic tends over time to a stationary state, which at typical parameter values corresponds to a low level of the relative number of cases $C_i = i/C$. However, at the initial stage of the disease, fluctuations of $C_i(t)$ of a large amplitude are observed, during which the number of cases reaches values comparable to the total population. As far as the results obtained for ODE, will they be observed in the PCA model?

The mean field model is constructed under the assumption of a uniform spatial distribution of viruses and individuals. This is achieved under conditions of strong mixing of viruses and individuals. Therefore, for $P_m \simeq 1$, both models should presumably give similar results. To test this assumption, let's compare the trajectories $C_i(t)$ of both models starting from the

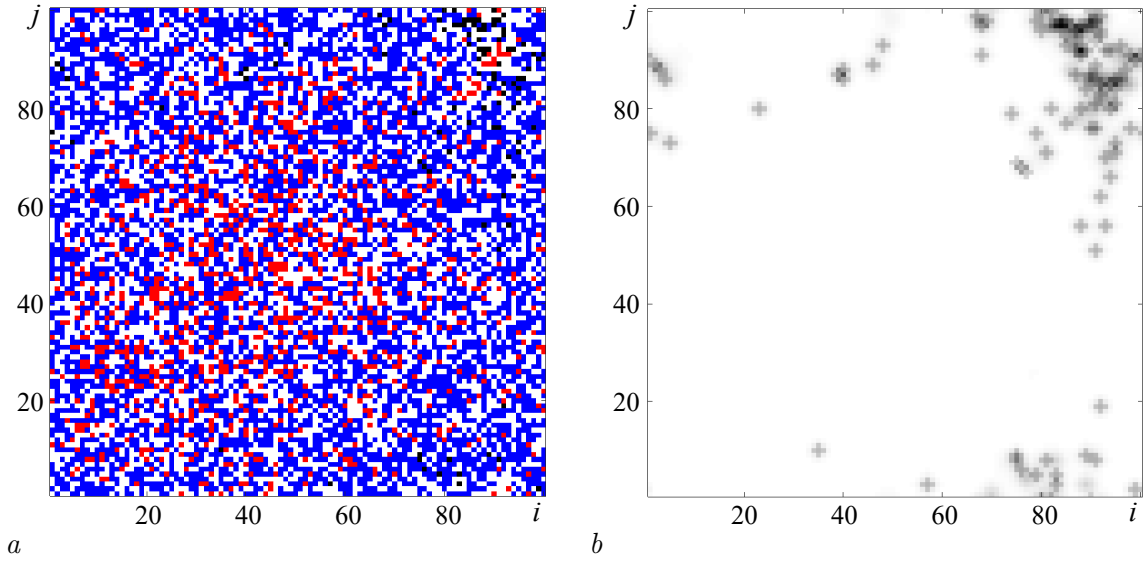

Fig. 1. Spatial distribution on the grid: *a* — of individuals (the state of the individual is marked with the color: «*S*» — red, «*I*» — black, «*R*» — blue) and *b* — viruses (the concentration of viruses is marked with shades of gray: the darker the color, the higher the concentration) (color online)

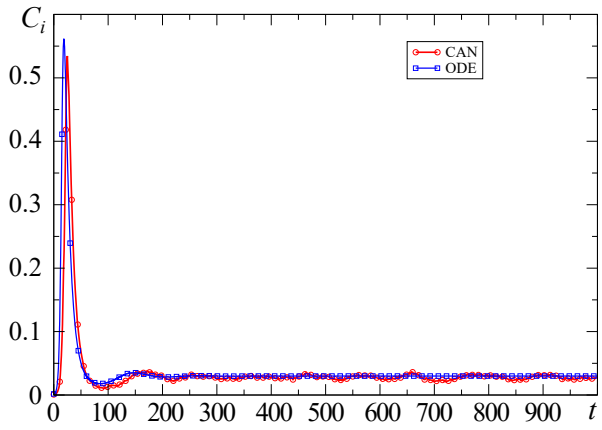

Fig. 2. Time dependence of the relative concentration of the diseased in the mean field (ODE) and cellular automata (CAN) models at $P_m = 1$ (color online)

same initial conditions and with equal values of all parameters. In the PCA model, we will use a complete mixing of individuals ($P_m = 1$). As calculations show, both models give similar results, examples of which are shown in Fig. 2. Here we see an almost complete coincidence of the time dependencies of $C_i(t)$. A similar correspondence is observed for other values of the system parameters (7). With a high population migration, the average field model adequately describes the dynamics of the disease and there is no need to involve a more complex model of PCA. However, with less migration (or its absence), the condition of spatial uniformity of the distribution of viruses and individuals ceases to be fulfilled. This should lead to a discrepancy in behavior both models. As shown below, with incomplete mixing, there is a qualitative similarity of the dynamics of both models with their quantitative divergence. In the absence of mixing, the existence of qualitatively new modes is possible. Let's take a closer look at what effects are observed in a spatially inhomogeneous environment.

5. The dynamics of the disease during migration changes

We will investigate how the dynamics in the PCA model changes when the probability of migration of individuals decreases from $P_m = 1$ to $P_m = 0$. This corresponds to the departure from the condition of uniform distribution of individuals in space. As initial conditions, we will choose the infection of a healthy population when one infected individual enters it. In the PCA model, this corresponds to a lattice filled with S cells with a given concentration C, in the center of which is placed one I-cell. In the course of modeling LCA, we will calculate time realizations for relative concentrations infected individuals $C_i(t)$. At the same time, both the dynamics of the transient process and the steady-state mode at $t \to \infty$ are of interest.

The dependences of $C_i(t)$ obtained as a result of numerical study are shown in Fig. 3, *a*. As can be seen from the graphs, when $P_m > 0$ the development of the epidemic follows the same qualitative scenario as in the mean field model, that is, through a sequence of decreasing «waves of infection» and transition to a stationary state: $i_s = \lim_{t\to\infty} i(t)$. At the same time, the final stationary value of i_s does not depend on the intensity of migration and coincides with the coordinates of the equilibrium state in the mean field model (7).

However, the value of P_m affects the characteristics of the transition process to a stationary state. As can be seen from Fig. 3, *a*, a decrease in migration leads to a significant decrease in the amplitude of the first « infection wave» from $C_i^{(1)} \simeq 0.5$ ($C_i^{(m)}$ — the maximum relative level of cases during the mth wave of infection) at $P_m \simeq 1$ to $C_i^{(1)} \simeq 0.1$ at $P_m \simeq 0.001$. At the same

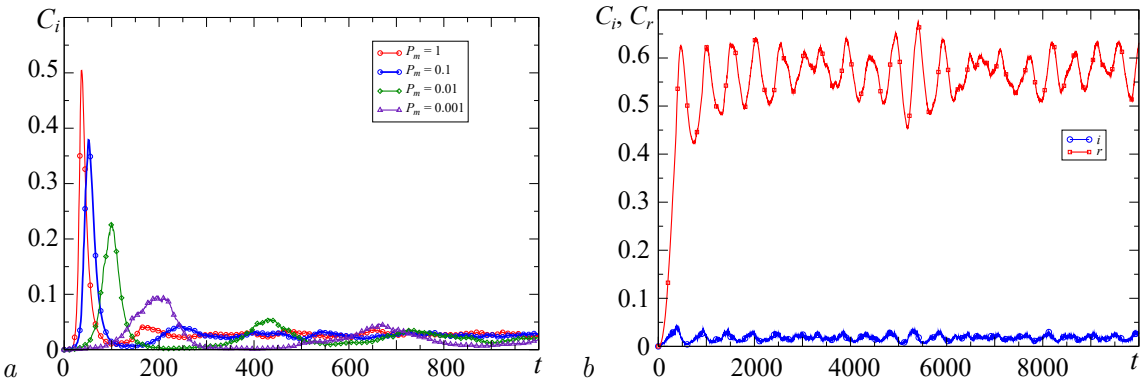

Fig. 3. Dynamics of the PCA model for different values of the migration parameter (a) and at the absence of migration (b) (color online)

time, there is no significant change in the amplitude of the second and subsequent «infection waves».

Dependency graphs $C_i^{(1)}(P_m)$ and $C_i^{(2)}(P_m)$ are shown in Fig. 4, *a*. Here we see that the amplitude of the first wave increases with an increase in P_m almost logarithmically, up to $P_m \simeq 0.4$. Then it stabilizes at a constant level. The amplitude of the second wave is almost independent of the magnitude of the migration. The growth of P_m, in addition to affecting the amplitude, leads to a change in the time characteristics of the transient process: «narrowing» of the first wave with $\Delta t^{(1)} \simeq 100$ up to $\Delta t^{(1)} \simeq 16$ and to a decrease in the average interval between consecutive waves of infection from $\Delta t_{1-2} \simeq 470$ up to $\Delta t_{1-2} \simeq 140$ (Fig. 4, *b*).

The presented figures clearly show that significant changes in the dynamics of the disease occur in the range of changes in the migration parameter $0 < P_m < 0.4$. After crossing the threshold value of $P_m \simeq 0.4$, marked with a dotted line, the increase in migration has almost no effect on epidemic processes.

Migration of individuals does not change the final level of cases in the population, but dramatically increases it at the initial stage and at the same time reduces the duration of the transition process. The analysis of dynamics at the initial level also indicates a change in the shape of $C_i(t)$ with a change in P_m.

To illustrate this effect, we present graphs of $C_i(t)$ at the stage of monotonous increase

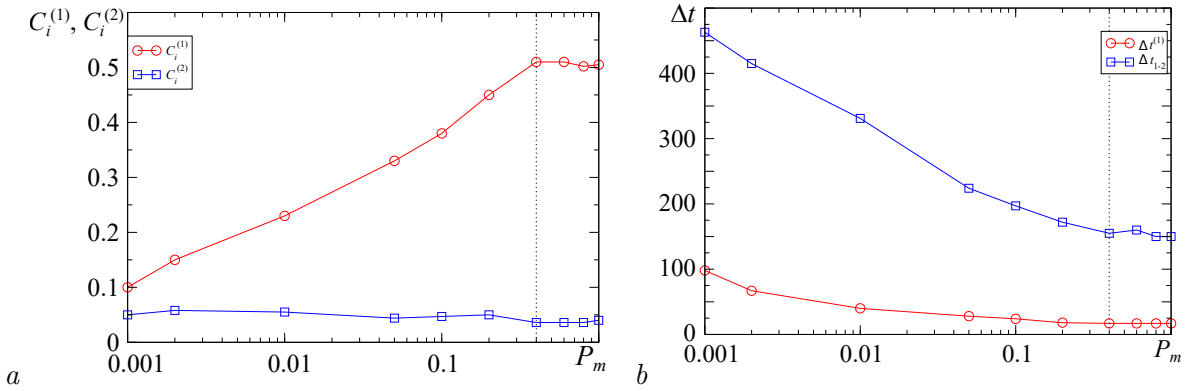

Fig. 4. a — — Dependence of the maximum level of the first ($C_i^{(1)}$) and the second ($C_i^{(2)}$) infection waves on P_m; b — dependence of the duration of the first infection wave ($\Delta t^{(1)}$) and the interval between the first and the second waves of infection (Δt_{1-2}) from P_m (color online)

in the number of infected during the «first wave» from $C_i(0) \simeq 0$ to the maximum value $C_i^{(1)}$ (Fig. 5). From the graphs we see that with $P_m = 1$ we have an «explosive», that is, an almost exponential increase in the number of cases. And at $P_m \ll 1$, the increase occurs more smoothly. At the same time, the smaller the migration, the more smoothly the disease increases.

Quantitatively, the rate of increase of $C_i(t)$ can be estimated using a polynomial approximation. As the calculations showed, the graphs in Fig. 5 are well approximated by power dependencies $C_i(t) = At^q$, where the order of q is determined by the value P_m. At the same time, the minimum degree of the polynomial is sufficient to approximate the experimental dependence. It can serve as a quantitative characteristic of the rate of infection growth at the initial stage. For example, to approximate the curve «$P_m = 1$» , it turned out to be sufficient to use a polynomial of the seventh degree, for $P_m = 0.1$ — fifth, etc. The smaller P_m, the lower the order of the approximating polynomial. In the absence of migration ($P_m = 0$), the increase in the number of cases at the initial stage occurs according to a law close to to the quadratic parabola.

At $0 < P_m \leqslant 1$, the dynamics of the PCA lattice qualitatively corresponds to the ODE model, although it differs quantitatively. As it was shown in [18], in the medium field model, the transition process from initial infection to a stationary state corresponds to the «winding» trajectory to a stable focus. We see a similar picture in the LCA. At the same time, the «decay decrement» of the transient process decreases with a decrease in the probability of migration. If the migration is completely «turned off» ($P_m = 0$), then «attenuation» will also disappear, and there will be continuous fluctuations in the system. Their example is shown in Fig. 3, *b*. The oscillation mode — is new in relation to the ODE model, in which it is not implemented. Thus, for $P_m = 0$, there is also a qualitative discrepancy between the dynamics of the ODE and the PCA.

6. Spatial distribution of cases in the PCA model

In the previous section, it was shown that the value of the migration parameter significantly affects the temporal dynamics of the disease. The reason for this should be the spatial heterogeneity of the distribution of cases, which increases with a decrease in migration. Let's consider the spatial distribution of infected people at different stages of the epidemic, starting from the moment of

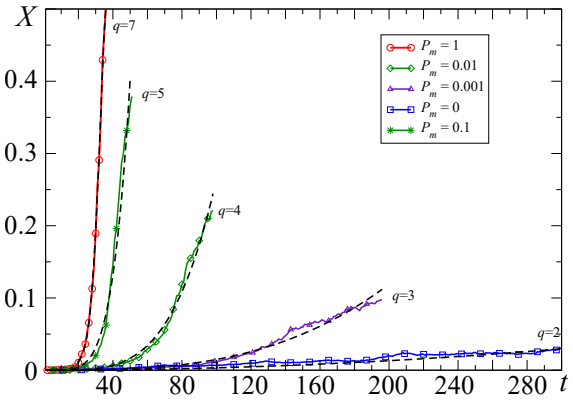

Fig. 5. Plots of the initial stage of the epidemic which correspond to a monotonic rise of the number of cases and their approximating functions $C_i(t) = At^q$, which are shown by dashed lines; the order of the approximating function is indicated near the corresponding curve (color online)

initial infection at $t = 0$. To do this, let's build a sequence of snapshots $V(i, j)$[3] for increasing moments of time at different values of P_m. The values of the remaining parameters and the initial conditions will remain the same as in the previous section.

In the absence of migration ($P_m = 0$), the temporary implementations of $i(t)$ and $r(t)$ represent a repetitive oscillatory process (Fig. 3, *b*). Suppose at time $t = 0$ one infected individual has penetrated into the population, which is localized in the center of the lattice. In this case, the initial distribution is a point that, due to diffusion, transforms into a small spot in the center of the lattice during the time $\Delta t = 50$ (Fig. 6, *a*). Further, during the development of the epidemic, by the time $t = 100$ (Fig. 6, *b*), this zone is gradually transformed into a ring area, which as t increases, it gradually spreads from the center to the periphery. This zone is the main focus of the epidemic, in the thickness of which most of the new infections occur. Inside the ring zone, the overwhelming number of individuals have already been ill and are immune. Outside there is an area susceptible to infection, which serves as a breeding ground for further infections. As the epidemic develops, the ring of infections gradually expands, covering more and more of the grid. At the same time, the rate of its expansion remains almost constant (see the curve «○» in fig. 7). Step by step, the infection ring expands more and more, captures almost the entire grid (Fig. 6, *c*), reaches its border (Fig. 6, *d*). Then the epidemic is on the wane. At the moment of $t \simeq 500$, the infection level becomes almost zero (Fig. 6, *e*). However, by this time the immunity in the central area of the lattice has disappeared. The remaining pinpoint foci of infection there become active centers for the following «infection rings» (Fig. 6, *f*). There is a second wave of infection that spreads in the absence of immunity and almost repeats the first one. The process is reproduced cyclically, creating almost periodic fluctuations in the level of infections.

[3]The distribution of viruses corresponds to the distribution of sick individuals, but it is more convenient to display.

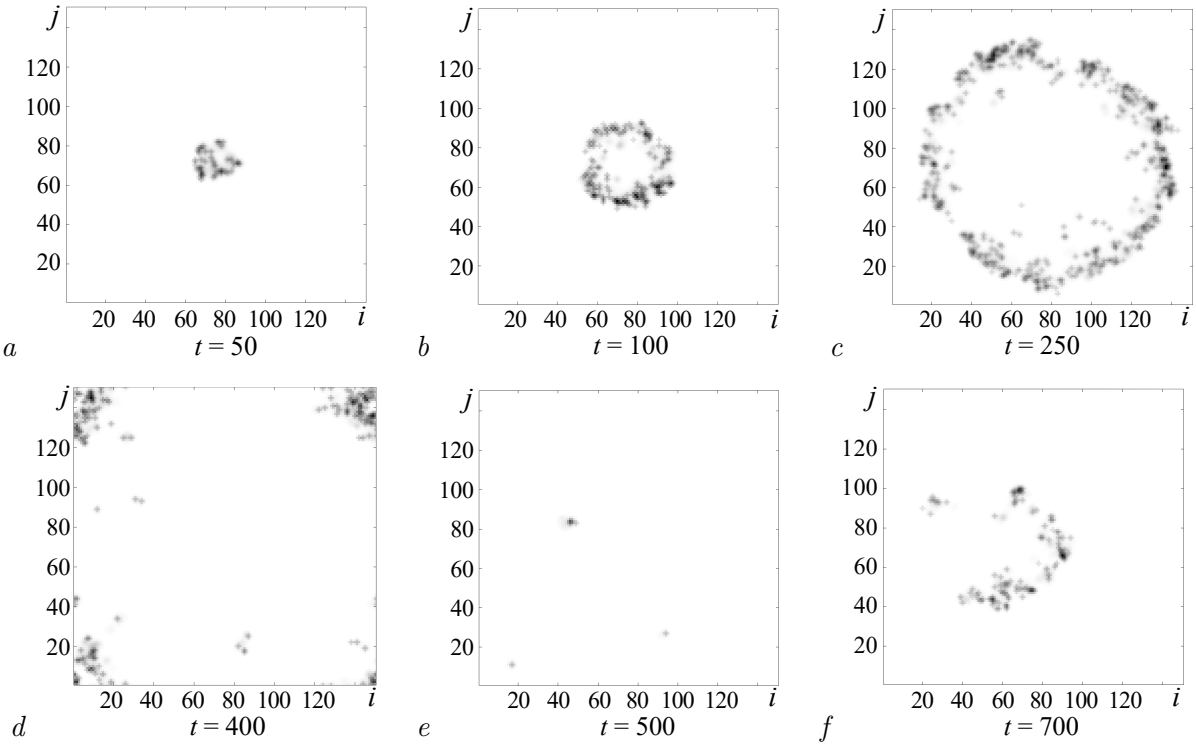

Fig. 6. Spatial distribution of viruses at different time moments at the absence of migration ($P_m = 0$)

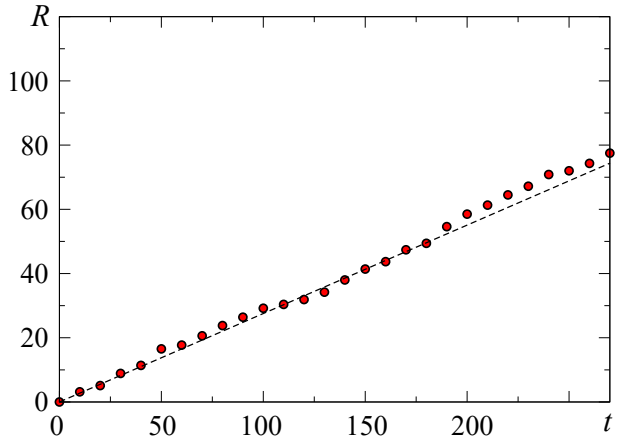

Fig. 7. Dependence of the outer radius «of the infection ring» (R) on time at $P_m = 0$ (color online)

If there is even a small migration ($P_m = 0.01$), the infection picture changes dramatically. Already at the initial stage , secondary foci «bud off» from the initial focus (Fig. 8, *a*), each of which is the source of its «ring of infections» (Fig. 8, *b*) and creates new foci of infection (Fig. 8, *c*). As a result, the growth of infection occurs simultaneously over the entire area of the grid. Already at $t = 100$, the maximum of the disease is reached when almost the entire lattice is covered with infection (Fig. 8, *d*). Then the wave is on the decline. By $t \simeq 250$, the disease stops, with the exception of the remaining single foci of infection. Subsequently, on their basis, according to the same scenario, a second wave of infection occurs. Since immunity in the population is still preserved by this time, the second wave grows slower than the first and reaches a much smaller value (Fig. 8, *f*). Subsequent waves are even less pronounced and gradually the disease reaches a stationary level. With more intensive migration, the qualitative picture does not change, but the infection processes accelerate: «explosive» is observed the growth of the disease, in which foci of infection appear simultaneously on the entire grid and the population very quickly becomes evenly infected. This case corresponds to an almost exponential increase in infection and its very high level at the peak of the disease.

Conclusion

The cellular SIRS+V model of the development of epidemic processes allows us to consider the temporal and spatial dynamics of the development of diseases, taking into account the spread of viruses and individuals in space due to diffusion and migration. The study showed that the spatial distribution of infection plays a decisive role in the development of the epidemic, changing the quantitative characteristics of the observed processes and leading to qualitatively new regimes. In the presence of a small migration in the PCA model, as well as in the ODE, there is transition to a stationary state through a sequence of fading «infection waves». However, the amplitude and duration of these waves turn out to be significantly dependent on the intensity of migrations: with increasing migration, the amplitude of the first wave of infection increases logarithmically, at the same time there is an «acceleration» of the transition process to a stationary state. The level of infections in the stationary state turns out to be the same as in the ODE model, and does not depend on migration. In the complete absence of migration of individuals in the cell model, there may be a mode of undamped oscillations, absent in the ODE model.

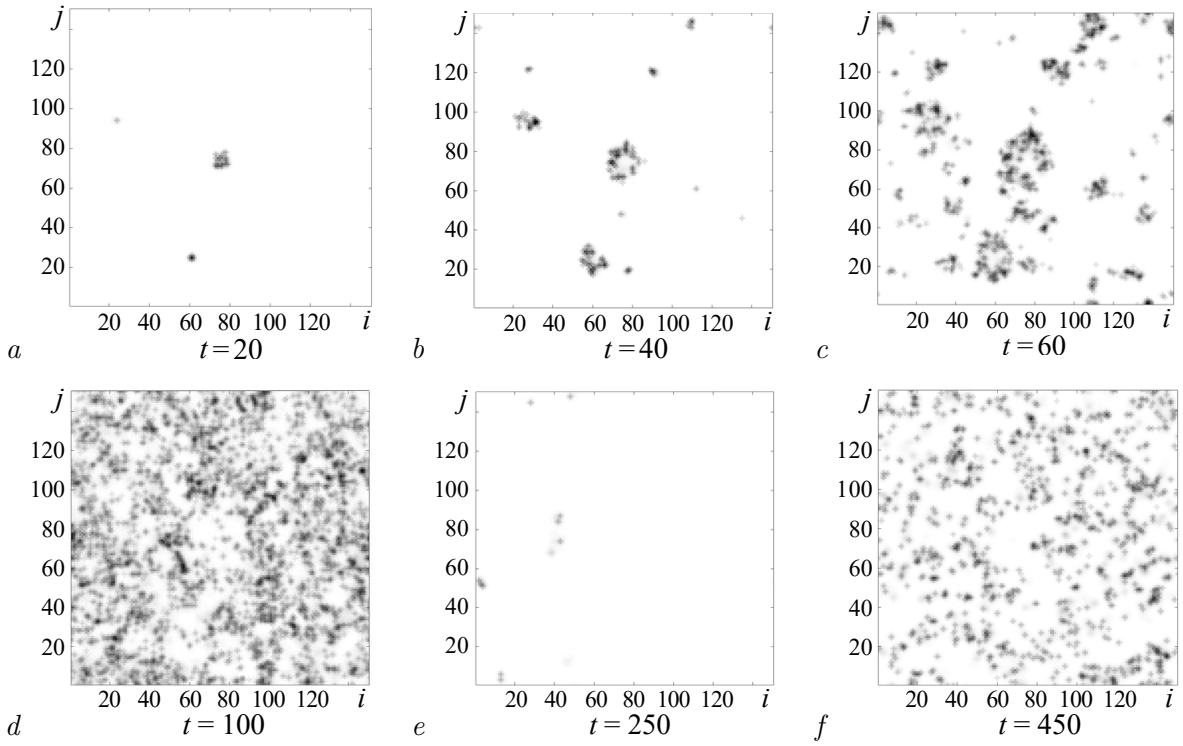

Fig. 8. Spatial distribution of viruses at different moments of time for small migration ($P_m = 0.01$)

References

1. Bailey NTJ. The Mathematical Approach to Biology and Medicine. London: John Wiley and Sons; 1967. 296 p. DOI: 10.2307/2982529.
2. Marchuk GI. Mathematical Models in the Immunology: Simulation Methods and Experiments. Moscow: Nauka; 1991. 276 p. (in Russian).
3. Hethcote HW. The mathematics of infectious diseases. SIAM Review. 2000;42(4):599–653. DOI: 10.1137/S0036144500371907.
4. Anderson RM, May R. Infectious Diseases of Humans: Dynamics and Control. Oxford: Oxford University Press; 1991. 768 p.
5. Serfling RE. Methods for current statistical analysis of excess pneumonia-influenza deaths. Public Health Reports. 1963;78(6):494–506. DOI: 10.2307/4591848.
6. Burkom HS, Murphy SP, Shmueli G. Automated time series forecasting for biosurveillance. Statistics in Medicine. 2007;26(22):4202–4218. DOI: 10.1002/sim.2835.
7. Pelat C, Boëlle PY, Cowling BJ, Carrat F, Flahault A, Ansart S, Valleron AJ. Online detection and quantification of epidemics. BMC Medical Informatics and Decision Making. 2007;7:29. DOI: 10.1186/1472-6947-7-29.
8. Kermack WO, McKendrick AG. A contribution to the mathematical theory of epidemics. Proc. R. Soc. Lond. A. 1927;115(772):700–721. DOI: 10.1098/rspa.1927.0118.
9. Bailey NTJ. The Mathematical Theory of Infectious Diseases and Its Applications. 2nd edition. London: Griffin; 1975. 413 p.
10. Boccara N, Cheong K. Automata network SIR models for the spread of infectious diseases in populations of moving individuals. Journal of Physics A: Mathematical and General. 1992;25(9): 2447–2461. DOI: 10.1088/0305-4470/25/9/018.
11. Sirakoulis GC, Karafyllidis I, Thanailakis A. A cellular automaton model for the effects

of population movement and vaccination on epidemic propagation. Ecological Modelling. 2000;133(3): 209–223. DOI: 10.1016/S0304-3800(00)00294-5.
12. Shabunin AV. SIRS-model with dynamic regulation of the population: Probabilistic cellular automata approach. Izvestiya VUZ. Applied Nonlinear Dynamics. 2019;27(2):5–20 (in Russian). DOI: 10.18500/0869-6632-2019-27-2-5-20.
13. Shabunin AV. Synchronization of infections spread processes in populations interacting: Modeling by lattices of cellular automata. Izvestiya VUZ. Applied Nonlinear Dynamics. 2020;28(4):383–396 (in Russian). DOI: 10.18500/0869-6632-2020-28-4-383-396.
14. Hamer WH. Epidemic disease in England – the evidence of variability and persistence of type. The Lancet. 1906;1:733–739.
15. Gopalsamy K. Stability and Oscillations in Delay Differential Equations of Population Dynamics. Dordrecht: Springer; 1992. 502 p. DOI: 10.1007/978-94-015-7920-9.
16. Perevaryukha AY. A continuous model of three scenarios of the infection process with delayed immune response factors. Biophysics. 2021;66(2):327–348. DOI: 10.1134/S0006350921020160.
17. Perevaryukha AY. Modeling of adaptive counteraction of the induced biotic environment du- ring the invasive process. Izvestiya VUZ. Applied Nonlinear Dynamics. 2022;30(4):436–455. DOI: 10.18500/0869-6632-2022-30-4-436-455.
18. Shabunin AV. Hybrid SIRS model of infection spread. Izvestiya VUZ. Applied Nonlinear Dynamics. 2022;30(6):717–731. DOI: 10.18500/0869-6632-003014.
19. Kobrinskii NE, Trahtenberg BA. Introduction to the Theory of Finite Automata. Moscow: Fizmatgiz; 1962. 405 p. (in Russian).
20. Toffoli T, Margolus N. Cellular Automata Machines: A New Environment for Modeling. Cambridge: MIT Press; 1987. 259 p.
21. Vanag VK. Study of spatially extended dynamical systems using probabilistic cellular automata. Phys. Usp. 1999;42(5):413–434. DOI: 10.1070/PU1999v042n05ABEH000558.
22. Provata A, Nicolis G, Baras F. Oscillatory dynamics in low-dimensional supports: A lattice Lotka–Volterra model. J. Chem. Phys. 1999;110(17):8361–8368. DOI: 10.1063/1.478746.
23. Shabunin AV, Baras F, Provata A. Oscillatory reactive dynamics on surfaces: A lattice limit cycle model. Phys. Rev. E. 2002;66(3):036219. DOI: 10.1103/PhysRevE.66.036219.
24. Tsekouras G, Provata A, Baras F. Waves and their interactions in the lattice Lotka–Volterra mode. Izvestiya VUZ. Applied Nonlinear Dynamics. 2003;11(2):63–71.
25. Boccara N, Cheong K. Critical behaviour of a probabilistic automata network SIS model for the spread of an infectious disease in a population of moving individuals. Journal of Physics A: Mathematical and General. 1993;26(15):3707–3717. DOI: 10.1088/0305-4470/26/15/020.
26. Benyoussef A, HafidAllah NE, ElKenz A, Ez-Zahraouy H, Loulidi M. Dynamics of HIV infection on 2D cellular automata. Physica A. 2003;322:506–520. DOI: 10.1016/S0378-4371(02)01915-5.
27. Fujisaka H, Yamada T. Stability theory of synchronized motion in coupled-oscillator systems. Progress of Theoretical Physics. 1983;69(1):32–47. DOI: 10.1143/PTP.69.32.
28. Yamada T, Fujisaka H. Stability theory of synchronized motion in coupled-oscillator systems. II: The mapping approach. Progress of Theoretical Physics. 1983;70(5):1240–1248. DOI: 10.1143/PTP.70.1240.